Pure & Appl. Chem., Vol. 62, No. 12, pp. 2269–2276, 1990.
Printed in Great Britain.

Dissolved and dispersed organic matter in natural waters. Progress by electroanalysis

Vera Žutić, Vesna Svetličić and Jadranka Tomaić

Center for Marine Research, Rudjer Bošković Institute, POB 1016, 41001 Zagreb, Yugoslavia

Abstract - Organic matter in seawater is chemically complex, physically heterogeneous and variable in time and space. Electrochemical techniques provide the most direct method to study trace levels of organic material in concentrated electrolyte solutions such as seawater.
We have identified a fraction of aquatic organic matter that was not amenable to analysis by conventional methods: fluid surface-active particles - droplets (d>0.5 μm). They are ubiquitous in productive surface waters, sea surface microlayer and mixing zones in estuaries ($\leq 10^9$ particles/l). The electrochemical methodology allows direct characterization of size, fluidity and surface conductance of individual particles through single coalescence events at the electrode/seawater interface.
The electrochemical characterization of organic matter at a natural fresh-water/seawater interface reveals a continuous transformation of biogenic dissolved organic matter into a highly hydrophobic surface-active material, both dissolved and dispersed, that forms a film.

INTRODUCTION

The largest pool of organic matter is contained in seawater. Organic matter in seawater is chemically complex, physically heterogeneous and variable in time and space (ref. 1). In estuarine mixing zones, additional complexity is encountered due to transformation of chemical and biological species under extreme salinity gradients (ref. 2).

A standard way of characterization of marine organic matter is either measurement of "dissolved" or "particulate" organic carbon (after filtration, 0.45 μm pore size), or determination of individual compounds or their classes, after a complex pretreatment of a seawater sample (ref. 3).

It has recently been shown that incomplete combustion resulted in a serious understimation of the global dissolved organic carbon pool (ref. 4) while pretreatments seriously alter organic species actually present in seawater.

Difficulties in physico-chemical speciation of organic constituents of seawater stem in part from low concentrations involved (total organic carbon is 0.3-3 mg C/l) and from complex nature of "dissolved" organic matter with molecular weights ranging from 16 to greater than 10^6 daltons. The classes of compounds present range from the simplest of hydrocarbons to complex biogeopolymers. Concentrations of carbohydrates, organic acids, proteins, lipids and other identified substances explain not more than 10% of the organic carbon in sewater (ref. 5). It has been suggested that major classes of biogenic organic materials form, under influence of high salt concentration, soluble surface-active complexes, glycolipid-protein, that transform to insoluble associates at natural interfaces (ref. 6,7).

Electrochemical techniques provide a direct approach to characterization of trace leves of organic material in seawater which is concentrated aqueous electrolyte solution (I = 0.7). Most commonly measured are phenomena of:

(1) complexation of electroactive metal ions by organic functional groups (complexing capacity) (ref. 8)

(2) adsorption of organic constituents (ref. 9,9a) at electrode/seawater interface (measurements of "surfactant activity" parameter we have introduced in 1973 (ref. 10)).

Mercury microelectrode serves as a probe and a model hydrophobic surface with controllable surface charge.

At short observation times, typical for the dropping mercury electrode (DME) $t_{DME} \lesssim 6$ s, dissolved organic molecules will randomly adsorb at the electrode/seawater interface (Fig. 1a) with surface coverage θ_a. The classical adsorption isotherms are appplicable.

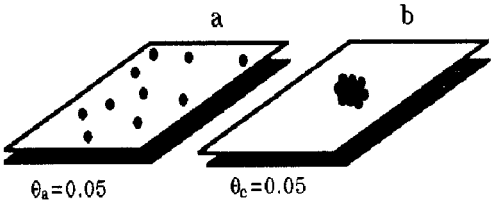

Fig. 1. Schematic presentation of electrode/seawater interface covered by: (a) randomly adsorbed molecules (θ_a = 0.05 and (b) condensed monolayer, θ_c = 0.05.

We expect that dispersed organic materials, if fluid, will transform to a condensed molecular layer (Fig. 1b) through phase transformation: droplet --> condensed monolayer. If so, surface coverage, θ_c identifies the fraction of the surface covered by the condensed film. Thus, θ_c = 0.05 means that 5% of the surface is covered by condensed film, while 95% is free (ref. 11,12). If the condensed phase is sandwiched between two liquids (fluid interface), it can be expected to have relatively few structural defects, if the film is also fluid. A two-dimensional film is not a separate phase in the thermodynamic sense, since it has no bulk properties.

THE ELECTROCHEMICAL METHOD

The electrochemical technique introduced here is basically chronoamperometry at the dropping mercury electrode (ref. 13) at potentials of streaming maximum (ref. 14,15) of 1 mM Hg(II) added to the sample. Suppression of streaming maxima by soluble surfactants provides a basis for their determination (a technique first introduced by Heyrovsky as "the adsorption analysis" (ref. 16). Increase of θ_a due to adsorption of organic molecules results in decrease of surface tension at the fluid interface. In chronoamperometric curve (Fig. 2) this manifests as a gradual, and highly reproducible decrease of current (Δi_a) of Hg(II) + 2e --> Hg(0) reaction, to the diffusion limited value, when θ_a approaches 1 (ref. 14,17).

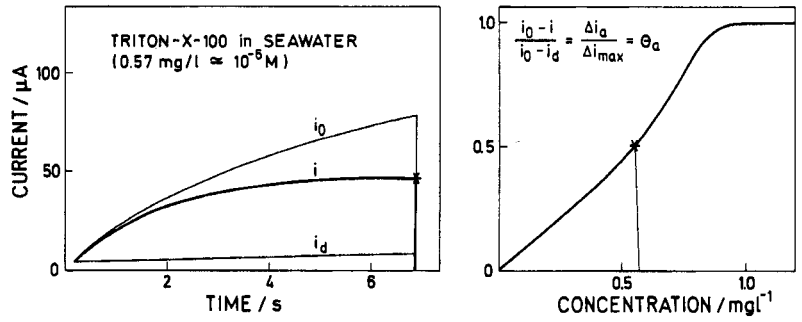

Fig. 2. I-t curves for reduction of 10^{-5} M Hg(II) in 10^{-4} M solution of Triton-X-100 in artificial seawater (E = -0.300 V *vs* Ag/AgCl). Curve i_o corresponds to organic-free seawater and electrode surface coverage θ = 0. Curve i_d corresponds to total suppression of the polarographic maximum which is achieved when θ_a approaches unity.

Calibration curve related the bulk concentration or equivalent surfactant activity of organic molecules with θ_m. The experimental methodology is described in detail in previous publications (ref. 18-21).

In diserpsion of fluid surfactants (e.g. methyl oleate, N = 1.1 x 10^8 particles/l, >1μm) : random arrival and attachment of fluid surface-active particles (SAP) result in characteristic perturbations (Fig. 3). If the same dispersion is filtered (0.45 μm pore size) the irregular oscillations disapppear completely, and the i-t curve of filtrate is identical to i_o.

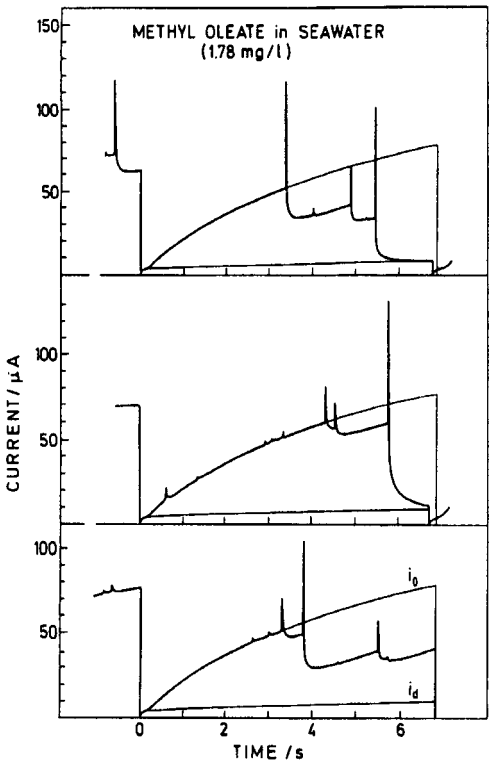

Fig. 3. i-t curves for reduction of 1 mM Hg(II) in the dispersion of 1.78 mg/l methyl oleate (N = 1.5 x 10^8 droplets/l) in artificial seawater (E = -0.300 V *vs* Ag/AgCl).
Curve i_o corresponds to organic-free seawater and electrode surface coverage θ_e = 0.
Curve i_d corresponds to total supression of the streaming maximum, when θ_e --> 1.

Each perturbation ends up with a decrease of current (Δi_e), which is proportional to the fraction of the electrode surface covered by condensed film, θ_e. Area of the electrode covered by the condensed film (A_e) at the moment of collision (t_m): $A_e = A_{DME} \times \theta_e$, where $A_{DME} = 4\Pi(3mt_m/4\Pi d_{Hg})^{2/3}$ (m is the flow rate of mercury and d specific density).

Each of perturbations, of variable amplitudes and frequency of appearance, corresponds to collision, attachment and spreading (coalescence) of a single SAP. Thus number of perturbations in an i-t curve corresponds to the number of coalescing SAP. The flux of SAP per unita area of DME is constant during the drop life. The mean number of parturbations per drop life is proportional to concentration of fluid particles in the bulk aqueous phase (ref. 22).

Coalescence of SAP takes place only within the range of potential where surfactant molecules are adsorbed. Collisions at more negative, or more positive, potentials do not lead to coalescence and SAP behave as inert particles (e.g. Al_2O_3), as there is no measurable perturbation of the current response (ref. 23,24).

In real systems, dissolved and dispersed organic material coexist. Oleic acid, sparingly soluble in artificial seawater (pH = 8.7) simulates such a system (Fig. 4).

Contribution from randomly adsorbed molecules (Δi_a) and coalesced particles (Δi_e) can be clearly distinguished. After filtration chronoamperometric curve corresponds to the unperturbed curve i (Fig. 4). Thus smaller aggregates, such as micelles, contribute to θ_a.

We conclude that, at mercury electrode/seawater interface oleic acid coexist in two immiscible surface states: randomly adsorbed and condensed.

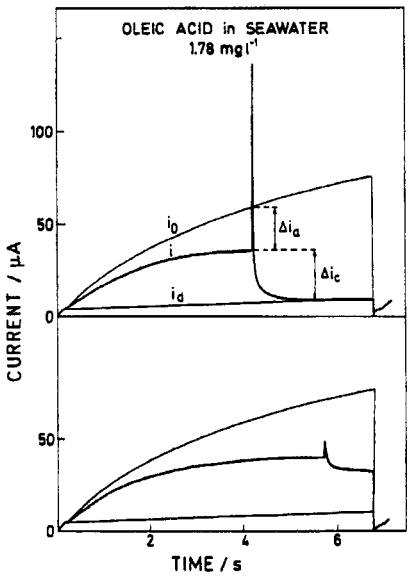

Fig. 4. i-t curves (two consecutive recordings) for reduction of 1 mM Hg(II) in presence of 1.78 mg/l oleic acid in artificial seawater (pH = 8.7).

The fraction of the mercury electrode/seawater interface covered by condesed film (θ_c) should behave as chemically modified electrode where the mechanism of Hg(II) reduction should not remain the same. The two extreme cases can be predicted:

(1) the organic film is insulator and as a consequence the charge transfer reaction: Hg(II) + 2 e^- --> Hg (Ø) bulk phase, should be blocked (ref. 25);

(2) the organic film is electronically conductive, and as a consequence the charge transfer reaction will proceed through formation of a new Hg(Ø) phase:

$$Hg(II) \xrightarrow[\text{nucleation}]{+\ 2\ e^-} Hg(Ø)\ \text{film}.$$

ANALYSIS OF INDIVIDUAL SAP IN MODEL DISPERSIONS

We shall now analyze the individual perturbations in i-t curves with increased time resolution. 1-heptadecene is fluid at ambient temperature and highly insoluble and surface-active in seawater. Coalescence signal for 1-heptadecene droplet is shown in Fig. 5.

By "coalescence signal" (ref. 26) we mean the segment of an i-t curve for 1 mM Hg(II) reduction during coalescence of an individual SAP at the mercury electrode.

Although the arrivals and collissions of SAP with the electrode are random events individual coalescences show highly reproducible general pattern consisting of:

(1) sudden increase in current (i_p)
(2) decrease in current (Δi_c) bellow the initial value i_o, and
(3) bell-shaped segment with a maximum, characterized by current i_m at time t_m.

We have interpreted sudden increase in current i_p as the initial attachment of the particle and the final decrease of faradaic current Δi_c as the result of spreading of surface-active material into the adsorbed surfactant layer at the electrode (ref. 23).

The rising portion of the bell-shaped segment can not be interpreted in terms of adsorption models since purely random transformation: SAP ---> adsorbed surfactant layer, would produce a monotonously falling transient. The rising portion of the bell-shaped segment is the evidence of a joint process of nucleation and growth of a new phase (ref. 27).

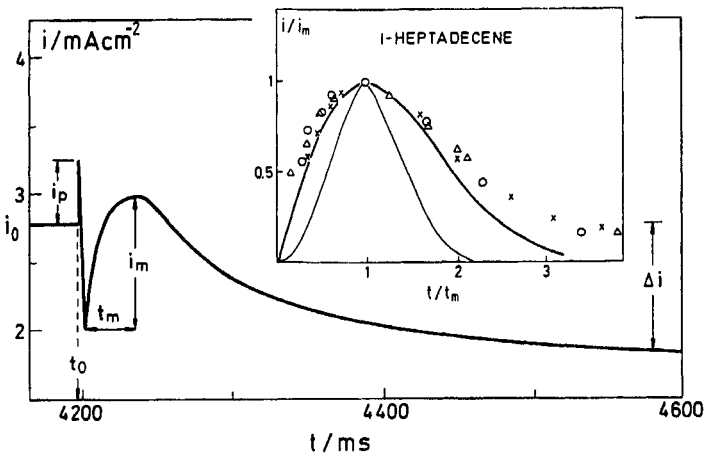

Fig. 5. Coalescence signal of a single surface-active particle in dispersion of 1.78 mg/l (N = 1.5 x 10^{8} particles/l) of 1-heptadecene in artificial SW. t_{∞} and i_{∞} denote time and current values at the onset of collision and attachment: t_m and i_m are used to construct the reduced variable plots for the analysis of nucleation mechanism: Δi is final net decrease of current.

For all recorded coalescence signals the charge density corresponding to the bell-shaped segment has a constant value of 424 $\mu C/cm^2$ (regression coefficient 0.962), when expressed per surface area of the organic film (as calculated from Δi_{∞}. This value is in a very good agreement with the theoretical charge for the formation of compact monolayer of elemental mercury, QHg = 403 $\mu C/cm^2$ (two-electron reduction and atomic radii, r = 0.159 nm).

It follows that the transformation of SAP to the condensed organic layer is accompanied by a fast two-dimensional (2D) nucleation and growth of compact monolayer of elemental mercury, with surface concentration Γ = (2.1 $\pm$ 0.2) x 10^{-9} g atom/cm^2, at the organic film/solution interface. The experimental data in Fig. 5 fit well 2D instantaneous nucleation and growth model for the formation of a new phase (ref. 28). This is surprising since it is known from literature that nucleation of mercury on foreign substrata, such as vitreous carbon (ref. 29) proceeds as a three-dimensional (3D) process. It is even more unexpected that the electrochemical reaction: Hg(II) + 2 e^- ---> Hg(0) occurs at the fraction of the mercury electrode covered by the organic film. This implies that the affinity of mercury atoms toward the organic film is high enough to overcome Hg-Hg interactions in 3D nuclei (i), to promote electron transfer through organic film (ii), and stabilize mercury atoms in the form of monolayer (iii).

In light of the above findings, the 2D phase, formed by coalescence of a single surface-active droplet at the model interface, is of molecular thickness as it allows efficient electron transfer for Hg(II) + 2 e^- ---> Hg(0) reaction, and also a compact molecular layer, since it is impermeable for mercury.

Electronic permeability of electroinactive and otherwise insulating molecular film of 1-heptadecene implies a strong interaction with mercury atoms arranged in the monolayer. A similar effect we have observed with monolayer of atomic sulphur that exhibits electronic conductivity when sandwiched between gold electrode and organic redox film (ref. 30).

In conclusion, from the response exemplified in Fig. 5 one can precisely determine the area of the organic monolayer and the amount of mercury(0) deposited at organic film/seawater interface.

Molecular structure of the organic film has no influence on the deposition of Hg(0) monolayer, as the same charge density (QHg = 424 $\mu C/cm^2$) was obtained for a number of model SAP (methyl oleate, oleic acid, squalene and olive oil) dispersed in aritificial seawater (Fig. 6a).

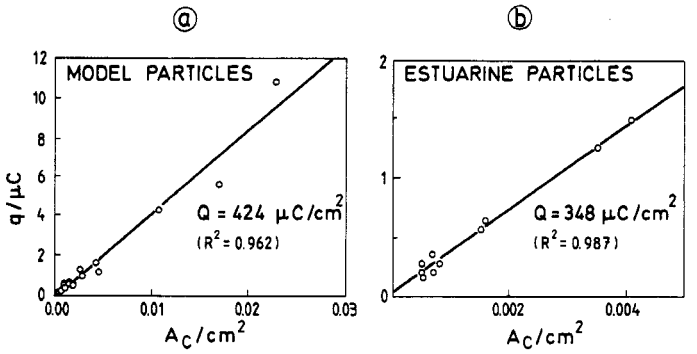

Fig. 6. Plot of charge for mercury(Ø) monolayer formation, q_{Hg}, *vs* area of the organic monolayer, $A_{\perp}$, calculated from coalescence signals recorded in: (a) model dispersion (1-heptadecene, squalene, methyl oleate, oleic acid and olive oil) in artificial seawater; (b) estuarine samples (Krka estuary, East Adriatic coast, 28 May 1987).

Although the deposition of mercury(Ø) monolayer is insensitive to the structure of molecules constituting organic film, the integral form of a coalescence signal (Fig. 7) reflects properties of SAP condensed phase . Size, fluidity, surface conductance and rate of spreading of SAP at the interface determine the height and width of the initial spike ($i_{\perp}$, Fig. 5) and the extent of overlap of spreading process with the nucleation of mercury(Ø).

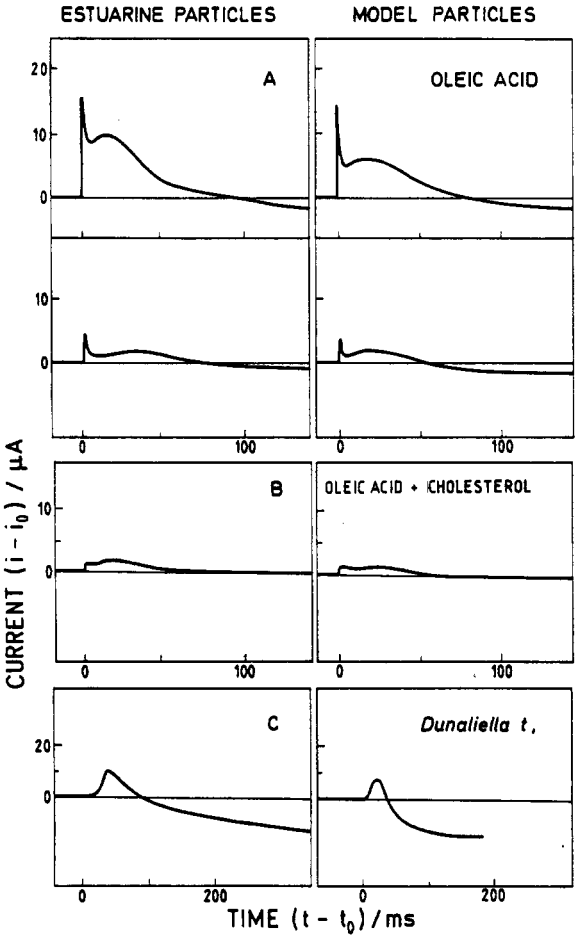

Fig. 7. Comparison of coalescence signal of estuarine SAP with signals of model SAP in artificial seawater. Estuarine samples were collected during spring cruise, 28 May 1987.

Thus, for example absence of initial spike in the coalescence signal of a phytoplankton cell (*Dunaliella tertiolecta*) suggests that the initial attachment is gradual and the deposition of Hg(Ø) occurs prior to

disintegration of the organism. Surface area of the mercury monolayer is in the range of 0.7 to 2.5 x 10^{-8} cm^2. This value is only a few times the geometrical surface area of the *Dunaliella tertiolecta* cell (volume = 421 ± 121 μm^3), and it could correspond to the cell membrane roughness, as seen by mercury atoms (ref. 31).

APPLICATION TO A NATURAL SYSTEM

Surface-active properties of the organic matter of fresh-water/seawater interface reflect a continuous transformation of dissolved organic matter (DOM) into a highly hydrophobic surface-active material both dissolved and disperse. The form of the AC responses (ref. 32) reveals presence of different surface-active groups, characteristic of polypeptides and polysaccharides, in a fairly constant proportion, and of the hydrophobicity comparable to lipids (ref. 33). We conclude that the surface-active material is present at the interface as a surface-active complex (ref. 6,7).

Hydrophobic interaction and orientation forces seem to be the most important mechanism of organic matter interaction at marine interface (Fig. 8). Unsaturated lipid molecules, micelles and larger aggregates were found to represent the most reactive surface-active material.

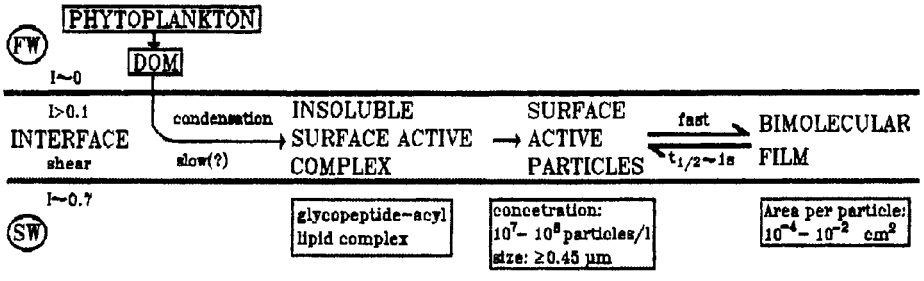

Fig. 8. Transformation of organic matter at the fresh-water (FW)/seawater (SW) interface of a stratified estuary (ref. 34).

We have identified a fraction of aquatic organic matter that was not amenable to analysis by conventional methods: fluid surface-active particles - droplets (d >0.5 μm). They are ubiquitous in productive surface waters, sea surface microlayers and mixing zones in estuarine ($N \leq 10^9$ particles/l). The electrochemical methodology allows direct characterization of size, fluidity and surface conductance of individual particles through single heterocoalescence events at the electrode/seawater interface.

Single coalescence events of all estuarine SAP studied at mercury/seawater interface show transformation into condensed monolayers, followed by 2D nucleation and growth of mercury(0) (Fig. 6b). A somewhat lower value for Q_{Hg} = 348 $\mu C/cm^2$ of the organic film *vs* 424 $\mu C/cm^2$ for model surfactants (Fig. 6a), might reflect presence of soluble surfactants in natural SAP.

Additional deposition of Hg(0) that accompanies the transformation of SAP into organic film probes the permeability (electronic and ionic) of the organic film formed. Moreover, Hg(0) can be considered a model hydrophobic pollutant.

Thus the strong interaction between natural SAP and Hg(0), that is not sensitive to molecular structure of the organic phase, might govern the interfacial behaviour of mercury in natural systems.

REFERENCES

1. F. Azam and B.C. Cho, Bacterial utilization of organic matter in the sea. In: Ecology of Microbial Communities, SGM 41, Cambridge University Press, pp. 261-281 (1987).

2. R.F.Z. Mantoura, Nature, 326, 579-580 (1987).

3. P.J. Wangersky, in: T.R.P. Gibb (ed.) Analytical Methods in Oceanography, Adv. Chem. Ser., 147, pp. 148-162, Washington (1975).

4. Y. Sugimura and Y. Suzuki, Mar. Chem., 24, 105-131 (1988).

5. E.K. Duursma and R. Dawson (eds.), Marine Organic Chemistry, 456 p., Elsevier, Amsterdam (1982).

6. J.S. D'Arrigo, J. Colloid Interface Sci., 100, 107-111 (1984).

7. W.R. Barger and J.C. Means, in: I. Sigelo and A. Hattori (eds.), Marine and Estuarine Geochemistry, pp. 45-67, Levis Publishers, Chelsea (1985).

8. H. van Leeuwen, R. Cleven and J. Buffle, Pure and Appl. Chem., 61, 266-274 (1988).

9. B. Ćosović, in: W. Stumm (ed.) Chemical Processes in Lakes, pp. 55-80, Wiley, New York (1985).

9a. B. Ćosović, in W. Stumm (ed.) Aquatic Chemical Kinetics, pp. 291-310, Wiley, New York (1990).

10. T. Zvonarić, V. Žutić and M. Branica, Thalassia Jugosl., 9, 65-74(1973)

11. R. Sridharan and R. de Levie, J. Electroanal. Chem., 201, 133-143 (1986)

12. R. de Levie, Chem. Rev., 88, 599-609 (1988).

13. A.J. Bard and L.R. Faulkner, Electrochemical Methods Fundamentals and Applications, pp. 136-172 Wiley, New York (1980).

14. V.G. Levich, Physicochemical Hydrodynamics, 700 p, Prentice-Hall, London (1962).

15. R. Aogaki, K. Kitazawa, K. Fueki and T. Mukaibo, Electrochim. Acta, 23, 867-874 (1978).

16. B. Gosmann and J. Heyrovsky, Trans. Electrochem. Soc., 59, 249 (1931).

17. B.G. Barradas and F.M. Kimmerle, J. Electroanal. Chem., 11, 163-170 (1966).

18. K.A. Hunter and P.S. Liss, Water Res., 15, 203-215 (1981).

19. V. Žutić, B. Ćosović, E. Marčenko, N. Bihari and F. Kršinić, Mar. Chem., 10, 505-520 (1981).

20. B. Ćosović, V. Žutić, V. Vojvodić and T. Pleše, Mar. Chem., 17, 127-139 (1985).

21. J.-C. Marty, V. Žutić, R. Precali, A. Saliot, B. Ćosović, N. Smodlaka and G. Cauwet, Mar. Chem., 26, 313-330 (1988).

22. J. Tomaić, T. Legović and V. Žutić, J. Electroanal. Chem., 259, 49-58 (1989).

23. T. Pleše and V. Žutić, J. Electroanal. Chem., 175, 290-312 (1984).

24. V. Žutić and J. Tomaić, Mar. Chem., 23, 51-67 (1988).

25. J. Lipkowski, C. Buess-Herman, J.P. Lambert and L. Gierst, J. Electroanal. Chem., 202, 169-189 (1986).

26. V. Svetličić and J. Tomaić, J. Electroanal. Chem., (in press).

27. E. Bosco and S.K. Rangarajan, J. Electroanal. Chem., 129, 25-51 (1971).

28. Southampton Electrochemistry Group, Instrumental Methods in Electrochemistry, pp. 283-316, Southampton (1985).

29. G. Gunaverdena, G. Hills, I. Montenegro and B. Scharifker, J. Electroanal. Chem., 138, 225-238 (1982).

30. V. Svetličić, V. Žutić, J. Clavilier and J. Chevalet, J. Electroanal. Chem., 233, 199-210 (1987).

31. V. Svetličić, V. Žutić and J. Tomaić, Mar. Chem., (in press).

32. B. Ćosović and V. Vojvodić, Mar. Chem., 28, 183-198 (1989).

33. V. Žutić, B. Ćosović, V. Vojvodić, J. Tomaić and G. Cauwet, Proc. X Int. Symp. Chemistry of Mediterranean, Primošten, pp. 51-52 (1988).